CBFA2T3-GLIS2 oncogenic fusion is sufficient for leukemic transformation

Quy Le (quyhale@gmail.com)
Fred Hutchinson Cancer Research Center
Brandon Hadland
Hutch
Jenny Smith
Fred Hutchinson Cancer Research Center
Amanda Leonti
Fred Hutchinson Cancer Research Center
Benjamin Huang
University of California San Francisco
Rhonda Ries
Fred Hutchinson Cancer Research Center
Tiffany Hylkema
Fred Hutchinson Cancer Research Center
Sommer Castro
Fred Hutchinson Cancer Research Center
Thao Tang
Fred Hutchinson Cancer Research Center
Cynthia Nourigat
Fred Hutchinson Cancer Research Center
LaKeisha Perkins
Fred Hutchinson Cancer Research Center
Larua Pardo
Hematologics, Inc.
Jay Sarthy
Fred Hutchinson Cancer Research Center https://orcid.org/0000-0001-5244-7865
Amy Beckman
University of Minnesota
Robin Williams
University of Minnesota
Rhonda Idemmili
University of Minnesota
Scott Furlan
Fred Hutchinson Cancer Research Center
Takashi Ishida
Fred Hutchinson Cancer Research Center
Lindsey Call
Fred Hutchinson Cancer Research Center
Shivani Srivastava
Fred Hutchinson Cancer Research Center
Anisha Loeb
Fred Hutchinson Cancer Research Center

Suzan Imren
Fred Hutchinson Cancer Research Center
Loken Michael
Hematologics, Inc.
Lisa brodersen
Hematologics, Inc.
Stanley Riddell
Fred Hutchinson Cancer Research Center
Katherine Tarlock
Fred Hutchinson Cancer Research Center
Irwin Bernstein
Fred Hutchinson Cancer Research Center and Universtiy of Washington https://orcid.org/0000-0003-0795-3392
Keith Loeb
Fred Hutchinson Cancer Research Center
Soheil Meshinchi
Fred Hutchinson Cancer Research Center

Biological Sciences - Article

Keywords: CBFA2T3-GLIS2 fusion, oncogenic fusion, leukemic transformation

Posted Date: August 12th, 2021

DOI: https://doi.org/10.21203/rs.3.rs-757279/v1

Abstract

Fusion oncoproteins are the initiating event in AML pathogenesis, although they are thought to require additional cooperating mutations for leukemic transformation. CBFA2T3-GLIS2 (C/G) fusion occurs exclusively in infants and is associated with highly aggressive disease[1-4]. Here we report that lentiviral transduction of C/G fusion is sufficient to induce malignant transformation of human cord blood hematopoietic stem and progenitor cells (CB HSPCs) that fully recapitulates C/G AML. Engineered CB HSPCs co-cultured with endothelial cells undergo complete malignant transformation with identical molecular, morphologic, phenotypic and disease characteristics observed in primary C/G AML. Interrogating the transcriptome of engineered cells identified a library of C/G fusion-specific targets that are candidates for chimeric antigen receptor (CAR) T cell therapy. We developed CAR-T cells directed against one of the targets, FOLR1, and demonstrated the pre-clinical efficacy against C/G AML while sparing normal hematopoiesis. Our findings underscore the role of the endothelial niche in promoting leukemic transformation of C/G-transduced CB HSPCs. Moreover, this work has broad implications for studies of leukemogenesis applicable to a variety of oncogenic fusion-driven pediatric leukemias, providing a robust and tractable model system to characterize the molecular mechanisms of leukemogenesis and identify biomarkers for disease diagnosis and targets for therapy.

Main

C/G expression transforms human CB HSPCs. CBFA2T3 (ETO2) is a member of the ETO family of transcription factors. Its fusion partner GLIS2 is a zinc finger protein regulated by the Hedgehog pathway. C/G AML is devoid of recurrent cooperating mutations[2,4,5], suggesting that the fusion might be sufficient for malignant transformation. To test this, we expressed the C/G fusion or GFP control in CB HSPCs (C/G-CB or GFP-CB) by lentiviral transduction and transplanted the transduced cells into NSG-SGM3 mice (Fig. 1a). Within 60 days of transplant, all mice (4/4) injected with C/G-CB cells developed florid leukemia, while all control mice (4/4) survived until study endpoint (Fig. 1b). Histology of the femur from C/G-CB xenograft mice revealed extensive leukemia with bone remodeling resembling the pathology observed in xenograft mice bearing C/G patient-derived leukemia cells (PDX, Fig. 1c; Supplemental Fig. S1). The malignant cells had a unique pattern of focal adhesion to neighboring cells characteristic of C/G AML. Flow cytometric analysis of marrow C/G-CB xenograft cells identified a malignant population that is of the RAM immunophenotype ($CD56^{hi}$, $CD45^{dim}$, and $CD38^{dim/-}$, Fig. 1d) previously reported in infants with C/G AML[6,7]. Immunohistochemistry further showed high expression of ERG and CD56 (markers associated with C/G AML[6-8]) in the mouse bone marrow indicative of malignant transformation, similar to the high CD56 expression in leukemia aggregates present in a bone marrow biopsy from a C/G patient (Fig. 1e).

To evaluate whether C/G imparts enhanced self-renewal to leukemia-initiating cells (LICs), we performed serial transplantation of C/G-CB cells. All mice from secondary (8/8) and tertiary (5/5) transplants also developed AML, with a median survival of 69 and 72 days, respectively (Fig. 1f). Bone marrow engraftment of C/G-CB cells was variable in these mice at time of symptomatic disease (5-70%, Fig. 1g); focal clusters of leukemia cells were present in the femur in all mice (Supplemental Fig. S1), resembling those of the primary transplant and the PDX model. Notably, there was immunophenotypic evolution during the serial transplants with expanded population of CD56+ cells (Fig. 1h). Similar observations were made in other tissues at necropsy (Extended Data Fig. 1a, b).

Acute megakaryocytic leukemia (AMKL) is a form of AML that is characterized by immature blasts expressing megakaryocytic markers CD41, CD42 or CD61[9]. Since AMKL is prevalent in C/G-positive patients[4], we assessed CD41 and CD42 expression on C/G-CB cells. Immunophenotype analysis revealed an aberrant megakaryocytic subset ($CD41^{-}CD42^{+}$) in the primary and subsequent serial transplantations (Fig. 1i; Extended Data Fig. 1c). Bertuccio et. al. previously identified a similar subpopulation whose gene expression most closely matched that of human C/G leukemia[10]. Monitoring CD41 and CD42 expression during serial transplantation showed an immunophenotypic evolution from $CD41^{-}CD42^{+}$ to the mature $CD41^{+}CD42^{+}$ megakaryocytic subsets (Fig. 1i, j, Extended Data Fig. 1c). Taken together, these results demonstrate that the expression of C/G induces transformation of CB HSPCs that faithfully recapitulates human C/G AMKL.

ECs promote leukemic progression *ex vivo*. Mounting evidence supports the role of the microenvironment in the leukemic process. Vascular niche endothelial cells (ECs), in particular, play a critical role in both normal and malignant hematopoiesis, contributing to maintenance and self-renewal of HSPCs as well as supporting leukemic progression, leukemia precursor survival and drug resistance[11-14]. Previous studies have demonstrated that human umbilical vein endothelial cells transduced with E4ORF1 virus (E4 ECs) support the expansion of CB HSPCs[15] and provide efficient conditions for long-term culture of primary AML precursors[13], thus effectively recapitulating the EC niche *ex vivo*. To assess whether ECs support leukemic transformation of C/G fusion, we cultured C/G-CB cells in E4 EC co-culture[15] or in myeloid-promoting conditions[16] (MC, Fig. 2a). C/G-CB cells expanded faster with prolonged lifespan in EC co-culture compared to MC, as determined by the cumulative number of GFP+ cells (Fig. 2b). In contrast, GFP-CB cells exhibited limited, short-lived proliferation reaching exhaustion after 3 weeks in either condition. Proliferation of C/G-CB cells declined after transfer to either an EC trans-well culture or in suspension culture (Fig. 2c), suggesting that the growth promoting effect of the ECs is mediated by direct contact and secreted factors.

The C/G fusion has been previously shown to confer self-renewal to hematopoietic progenitors[2,8]. This property in C/G-CB cells was further enhanced by EC co-culture. At 6 weeks, C/G-CB cells in EC co-culture formed significantly more megakaryocytic colonies than C/G-CB cells grown in MC or C/G-GFP cells grown in either condition. Strikingly, after 12 weeks C/G-CB cells cultured in EC co-culture produced a large number of megakaryocytic colonies (Fig. 2d), demonstrating long lived self-renewal of the C/G-CB cells co-cultured with ECs.

To determine whether the EC niche promotes the generation and propagation of LICs, we evaluated the engraftment of C/G-CB cells expanded on ECs or in MC following 3, 6, 9 and 12 weeks of culture. Remarkably, C/G-CB cells cultured in EC co-culture at each time point exhibited robust engraftment that progressed to frank leukemia *in vivo* (Fig. 2e, Extended Data Fig. 2), demonstrating that EC co-culture promotes long-term maintenance of functional LICs. C/G-CB cells grown in the MC also induced leukemia from 3- and 6-week cultures but then became senescent at 9 and 12 weeks, suggesting limited preservation of the LICs.

To monitor leukemic evolution, we assessed the expression of the RAM immunophenotype and AMKL markers on C/G-CB cells from EC co-culture and MC. C/G-CB cells in EC co-culture constituted an almost homogeneous population that expressed the RAM immunophenotype, whereas only a subset was detected in the MC at week 6 (Extended Data Fig. 3a). A high percentage of CD56+ cells was maintained in EC co-culture for 6-12 weeks (Fig. 2f). Emergence of the aberrant $CD41^{-}CD42^{+}$ subset occurred by week 3 in both culture conditions, albeit more prominently in EC co-culture (Fig. 2g, Extended Data Fig. 3b), then progressed to the more mature immunophenotype. Morphological evaluation showed megakaryocytic features among C/G-CB cells in both culture conditions (Extended Data Fig. 3c). These results were reproduced in a separate experiment with CB HSPCs from another donor (Extended Data Fig. 4). Thus, EC co-culture supports the development of C/G-transformed CB HSPCs that recapitulate the series of immunophenotypic changes associated with transformation in primary C/G AML.

Fidelity of engineered cells to C/G AML. To determine the fidelity of transformation to primary leukemia, we performed RNA-sequencing of C/G-CB cells cultured with ECs or in MC. Remarkably, unsurpervised clustering analysis demonstrated that the C/G-CB cells from weeks 6 and 12 in EC co-culture clustered with primary C/G-positive patient samples, but not C/G-CB cells cultured in MC nor GFP controls (Fig. 2h). This suggested that the signaling pathways that are aberrantly dysregulated in primary C/G leukemia are faithfully recapitulated in C/G-CB cells co-cultured with ECs. Further transcriptome analysis revealed up-regulation of *ERG* and *BMP2*, downstream genes previously shown to be strongly upregulated in C/G AML[2,8], and down-regulation of erythroid-megakaryocyte differentiation gene *GATA1*[17-21], also down-regulated in C/G AML[8], in both EC co-culture and MC (Extended Data Fig. 5a, top). However, there were significant differences in the global expression profiles of C/G-CB cells from EC co-culture compared to MC (Fig. 2i).

To determine the effects of ECs on malignant transformation, we assessed the status of the WNT, HEDGEHOG and TGF-beta pathways known to be dysregulated in C/G leukemia[2,4]. These pathways were highly enriched in C/G-CB cells grown in EC co-culture but not in MC (Extended Data Fig. 5a, bottom). We previously demonstrated that a number of cell adhesions and integrins are upregulated in C/G leukemia[4]. A majority of these genes were upregulated in C/G-CB cells independent of the culture condition (Extended Data Fig. 6a), suggesting this pathway is determined by the fusion and not the microenvironment. The expression of cell

adhesions and integrins presumably contributes to the focal distribution and adherent morphology identified in the C/G-CB xenograft mice (Fig. 1c).

Gene Set Enrichment Analysis (GSEA) also revealed that C/G and HSC signature genes, previously identified to be associated with C/G AML[4,8], were both significantly enriched in C/G-CB cells grown in EC culture relative to MC (Fig. 2j; Extended Data Fig. 6b, c). Hippo signaling pathway and tight junction are other C/G-specific pathways [see Ref.[4]] that were also significantly enriched in the C/G-CB cells in EC co-culture compared to MC (Extended Data Fig. 5b). Together, these results suggest that ECs induce transcriptional programs that synergize with the fusion to recapitulate the primary leukemia.

Upregulation of FOLR1 therapeutic target. Although CAR T therapy has proven successful in treating B-ALL, immunotherapeutic targeting of AML remains a challenge given significant overlap of target antigens expressed on AML and normal hematopoietic cells. Our expansive target discovery effort through TARGET and Target Pediatric AML (TpAML) has identified a library of AML-restricted genes (expression in AML, silent in normal hematopoiesis) in one or more AML subtypes, including C/G AML (607 genes, Fig. 3a; Extended Data Fig. 7). Of these, 42 were upregulated in both C/G AML and in C/G-CB cells cultured with ECs, representing C/G fusion-linked genes. Eighteen of these encode proteins that localize to the plasma membrane, of which seven C/G fusion-specific CAR targets (*FOLR1, MEGF10, HPSE2, KLRF2, PCDH19,* and *FRAS1,*) were identified to be highly expressed in C/G patients and in C/G-CB cells but entirely silent in normal hematopoesis (Fig. 3b, c).

We prioritized FOLR1 for further development given its existing record as a target in solid tumors[22]. We confirmed *FOLR1* transcript expression by qPCR (Supplemental Fig. 2). Flow cytometric analysis of primary AML cells showed that FOLR1 was expressed on AML blasts but not on normal lymphocytes, monocytes, and myeloid cells within individual patients (Fig. 3d, e). Surface FOLR1 protein was detected in C/G-CB cells as early as 6 weeks of EC co-culture, progressing to near uniform expression by week 12 (Fig. 3f, g).

Targeting C/G AML with FOLR1 CAR T. The evidence that FOLR1 is causally linked to the C/G fusion and uniquely expressed in AML blasts suggested that targeting FOLR1 may provide a specific strategy to eliminate C/G leukemia without impacting normal hematopoiesis. To evaluate the therapeutic potential of targeting FOLR1, we generated a FOLR1-directed CAR using anti-FOLR1 binder (Farletuzumab), IgG4 intermediate spacer and 41-BB/CD3zeta signaling domains (see Methods). We tested the target specificity of FOLR1-directed CAR T cells against FOLR1-positive (C/G-CB, WSU-AML, Kasumi-1 *FOLR1+*) and FOLR1-negative (Kasumi-1) cells. CD8 FOLR1 CAR T cells demonstrated cytolytic activity against FOLR1 positive but not FOLR1 negative cells (Fig. 4a). Furthermore, both CD8 and CD4 FOLR1 CAR T cells produced higher levels of IL-2, IFN-γ, and TNF-α and proliferated more robustly than did unmodified T cells when co-incubated with FOLR1 positive but not FOLR1 negative cells (Fig. 4b, c). These results indicate highly specific reactivity of FOLR1 CAR T cells against AML cells expressing FOLR1.

We next investigated the *in vivo* efficacy of FOLR1-directed CAR T cells. In C/G-CB, WSU-AML, and Kasumi-1 *FOLR1+* xenograft models, treatment with FOLR1 CAR T cells induced leukemia clearance, while disease progression occurred in all mice that received unmodified T cells (Fig. 4d; Extended Data Fig. 8a). Leukemia clearance was associated with expansion of CAR T cells in the peripheral blood of C/G-CB and WSU-AML xenografts (Extended Data Fig. 8b). Importantly, treatment with FOLR1 CAR T cells significantly extended the median survival in mice bearing C/G-CB, WSU-AML, Kasumi-1 *FOLR1+* leukemias, respectively (Extended Data Fig. 8c). Activity of FOLR1 CAR T cells *in vivo* was target specific, as they did not limit the leukemia progression nor extend the survival of Kasumi-1 xenografts (Fig. 4d, Extended Data Fig. 8c).

To determine whether FOLR1 is expressed on normal HSPCs, we characterized FOLR1 expression in CB CD34+ samples from three healthy donors. FOLR1 expression was entirely silent in HSPC subsets (Extended Data Fig. 9a-c). Consistent with lack of expression, no cytolytic activity was detected against HPSCs after 4-hour co-incubation with CAR T cells (Extended Data Fig. 9d). Moreover, FOLR1 CAR T cells did not affect the self-renewal and multilineage differentiation capacity of normal HSPCs as compared to unmodified control T cells (Extended Data Fig. 9e), whereas significant eradication of colonies were detected in the C/G-CB cells (Extended Data Fig. 9f). Taken together, these results suggest that FOLR1 CAR T can eradicate C/G AML cells without compromising normal HSPCs and may be a promising therapy for C/G AML.

Discussion

Previous attempts to generate overt leukemia from C/G-transduced murine marrow hemopoietic cells have not been successful[2,23], leading to the notion that cooperating mutations are required for leukemic transformation. In this study, we demonstrate that the C/G oncogenic fusion is sufficient to transform human CB HSPCs that faithfully recapitulates the transcriptome, morphology and immunophenotype of C/G AML observed in infants as well as highly aggressive leukemia in xenograft models. We further demonstrate that direct interactions with EC niche are required for malignant transformation by this fusion protein. These results demonstrate that oncogenic fusions may be sufficient to induce frank AML phenotype given the appropriate developmental milieu (CB HSPCs) and the permissive microenvironment (EC niche). This contrasts with the widely accepted "cooperative" model of AML requiring synergy between a class II (fusion) and class I (SNVs) variants for recapitulating the AML phenotype[24].

Progress in elucidating mechanisms of disease and development of novel therapies for the C/G AML cohort is currently limited by a lack of relevant model systems that accurately recapitulate human disease. The EC co-culture platform we developed overcomes this barrier and recapitulates the vascular EC niche that supports malignant transformation, self-renewal and LIC propagation in vitro. This platform is thus suited to interrogating AML-niche interactions and identifying novel therapeutic targets for C/G, and it should be extended to studies with other oncogenic fusions.

Finally, the results presented here address a fundamental challenge in immunotherapy for AML, as AML-restricted targets have been elusive. By integrating transcriptomics of primary C/G AML and engineered CB cells, we have now identified seven C/G fusion-specific genes that represent potential high-value targets and validated one of them, FOLR1, by showing that FOLR1-direct CAR T effectively eradicates C/G AML cells while sparing normal HSPCs. These results provide the pre-clinical foundation for further evaluation of FOLR-directed CAR T in clinical trials for the treatment of C/G AML.

Material And Methods

Animals

NOD/SCID/$\gamma c^{-/-}$ (NSG) and NOD.Cg-*Prkdc*^{scid} *Il2rg*^{tm1Wjl} Tg(CMV-IL3,CSF2,KITLG)1Eav/MloySzJ (NSG-SGM3) mice were obtained from the Jackson Laboratory, housed and bred at the Fred Hutchinson Cancer Research Center (FHCRC) (Seattle, WA). For all experiments, 6–10-week-old age-matched females were randomly assigned to experimental groups. Mice transplanted with engineered CB or AML cell lines were monitored and euthanized when they exhibited symptomatic leukemia (tachypnea, hunchback, persistent weight loss, fatigue or hind-limb paralysis). Experiments were performed after approval by Institutional Animal Care and Use Committee (protocol #51068) and in accordance with institutional and national guidelines and regulations.

Primary Specimens

Human umbilical cord blood samples were obtained from normal deliveries at Swedish Medical Center (Seattle, WA). Frozen aliquots of AML diagnostic bone marrow samples were obtained from the Children's Oncology Group. Cells were thawed in IMDM supplemented with 20% FBS and 100 U/mL DNaseI (Sigma, Cat#D5025). A bone marrow biopsy from a C/G patient was obtained from a patient treated at the University of Minnesota Masonic Children's Hospital. Healthy donor T cells were obtained from Bloodworks Northwest (Seattle, WA). We confirmed these cells lacked infections agents (EBV, HCMV, Hepatitis A, Hepatitis B, Hepatitis C, HHV 6, HHV 8, HIV1, HIV2, HPV16, HPV18, HSV1, HSV2, HTLV 1, HTLV 2, and *Mycoplasma sp*) through IDEXX Bioanalytics (West Sacramento, CA). All specimens used in this study were obtained after written content from patients and donors. The research was performed after approval by the FHCRC Institutional Review Board (protocol #9950). The study was conducted in accordance with the Declaration of Helsinki.

Cell lines

M07e (DSMZ, Cat# ACC104), WSU-AML (BioIVT, Cat# HCL-WSUAML-AC), Kasumi-1 (ATCC, Cat# CRL-2724) cell lines were maintained per manufacturer's instructions. We engineered Kasumi-1 *FOLR1*+ cell line by transducing Kasumi-1 cells with a lentivirus containing the *FOLR1* transgene driven by the EF1a promoter (Genecopoeia, Cat# LPP-C0250-Lv156-050). Jurkat Nur77 reporter cells[25] were maintained in RPMI supplemented with 20% FBS and 2 mM L-Glutamine.

Constructs and Lentivirus production

The MSCV-CBFA2T3-GLIS2-IRES-mCherry construct was a gift from Dr. Tanja Gruber (Department of Oncology, St. Jude Children's Research Hospital, Memphis, Tn, Ref[2]). The *C/G* fusion gene from this construct and the MND promoter were inserted into pRRLhPGK-GFP lentivirus vector[26] as described in Ref.[4].

CAR constructs containing IgG4 short, intermediate and long spacers are previously described in Ref.[27]. The VL and VH sequences from Farletuzumab were used to construct the anti-FOLR1 scFv with VL/VH orientation using G4SX4 linker. Anti-FOLR1 scFv DNA fragment was human codon optimized and synthesized by IDT gBlock gene fragment and cloned into the CAR vectors with NheI and RsrII restriction sites upstream of the IgG4 spacer.

Farletuzumab scFv:

DIQLTQSPSSLSASVGDRVTITCSVSSSISSNNLHWYQQKPGKAPKPWIYGTSNLASGVPSRFSGSGSGTDYTFTISSLQPEDIATYYCQQWSS
YPYMYTFGQGTKVEIKGGGGSGGGGSGGGGSGGGGSEVQLVESGGGVVQPGRSLRLSCSASGFTFSGYGLSWVRQAPGKGLEWVAMISS
GGSYTYYADSVKGRFAISRDNAKNTLFLQMDSLRPEDTGVYFCARHGDDPAWFAYWGQGTPVTVSS

Lentivirus particles were produced in 293T cells (ATCC, Cat#CRL-3216). 293T cells were transfected with transfer vector, viral packaging vector (psPAX2), and viral envelope vector (pMD2G) at 4:2:1 ratio using Mirus 293Trans-IT transfection agent (Mirus, Cat# MIR2700) as directed by manufacturer's protocol. Viral particles were collected each day for 4 days post transfection, filtered through 0.45 µm membrane (Thermo Fisher; Cat NAL-166-0045) and concentrated (overnight spin at 4ºC, 5000rpm) before use.

Transduction of cord blood CD34+ cells

CB samples were processed with red blood cell lysis buffer and enriched for CD34+ cells using CliniMACS CD34 MicroBeads (Miltenyi Biotec, Cat# 130-017-501). CB CD34+ cells were then seeded onto retronectin (5 ug/mL, Takara, Cat#T100A) + Notch ligand Delta1 (2.5 ug/mL, Ref[28]) coated plates overnight in SFEM II medium (StemCell Technologies, Cat# 09650FH) containing 50ng/mL stem cell factor (SCF, StemCell Technologies, Cat# 78062), 50ng/mL thrombopoietin (TPO, StemCell Technologies, Cat# 78210) and 50ng/mL Fms-like tyrosine kinase 3 ligand (FLT3L, StemCell Technologies, Cat# 78009). Cells were transduced the following day with the C/G construct at an MOI of 200 or GFP control construct at MOI of 50. Transduced cells were grown on Notch ligand at 37ºC in 5% CO_2 for 6 days then sorted for GFP+ cells. Sorted GFP+ cells were either transplanted into NSG-SGM3 mice at 200,000 cells per mouse or placed in EC co-culture or myeloid promoting condition (MC, see Ref.[16] and below) for long term culture at 75,000 cells per 6-well. In a subsequent experiment using a CB CD34+ sample from another donor (CB 2, see Extended Fig. 4), transduced cells were grown on Notch ligand for 2 days prior to placement in EC co-culture or MC plating at 100,000 cells per 12-well.

Long term culture of transduced cord blood CD34+ cells

Transduced cells were placed in either EC co-culture with SFEM II medium supplemented with 50ng/mL SCF, 50ng/mL TPO, 50ng/mL FLT3L, and 100U/mL Pen/Strep, or MC containing Iscove's Modified Dulbecco's Medium (IMDM, Gibco 12-440-053) supplemented with 15% fetal bovine serum (FBS, Corning, 35-010-CV), 100U/mL Penicillin-Streptomycin (Pen/Strep, Gibco, 15-140-122), 10ng/mL SCF, 10ng/mL TPO, 10ng/mL FLT3L, 10ng/mL IL-6 (Shenandoah Biotechnology, Cat#100-10), and 10ng/mL IL3 (Shenandoah, Cat#100-80). For EC co-cultures, human umbilical vein endothelial cells (HUVECs) transduced with E4ORF1 construct (E4 ECs) were propagated as previously described[13,29]. One day prior to co-culture, E4 ECs were seeded into 6-well or 12-well plates at 800,000 or 300,000 cells per well, respectively, and cultured in medium 199 (Biowhittaker #12-117Q) supplemented with FBS (20%, Hyclone, Cat#SH30088.03), endothelial mitogen (Biomedical Technologies, Cat#BT203), Heparin (Sigma, Cat# H3149), HEPES (Gibco, Cat# 15630080), L-Glutamine (Gibco, Cat# 25030), and Pen/Strep. After 24 hours, E4 ECs were washed with PBS and cultured with transduced CB cells in media described above. Transduced CB cells in either culture condition were propagated with fresh media and E4 ECs replaced every week until cells stopped proliferating. Three-to-twenty percent of the cultures were re-plated each week for long-term culture.

We confirmed *C/G* and *FOLR1* expression in engineered cells over weeks in culture using RT-PCR (Supplemental Fig. 3). Tranduced CB cells were sorted for GFP+ cells on an FACSAria II using FACSDiva Software (BD Biosciences). DNA and RNA from sorted cells

were extracted with AllPrep DNA/RNA/miRNA Universal Kit using the QIAcube platform (QIAGEN). Expression of the fusion transcript in GFP+ cells was confirmed by RT-qPCR TaqMan assay and QuantStudio 5 real-time PCR system using the primers: Forward 5-CCCTGACGGTCATCAACCA-3, Reverse 5-CACCATCCAAATAGCGCAGTG-3, and TaqMan probe 5-[FAM]-CAGCGAGGACTTCCAG-[MGB]-3. *FOLR1* expression was determined using RT-qPCR TaqMan assay (Hs01124177_m1, cat# 4331182).

Cell surface analysis

For xenograft CB cells, mouse bone marrow, peripheral blood, spleen, and liver were harvested at necropsy and processed with red blood cell lysis buffer. Spleen and liver were processed into cell suspension with glass slides and passed through a 70-um cell strainer. CB cells in EC co-culture and MC were harvested after vigorously pipetting to resuspend CB cells. CB cells from processed mouse tissues and cultures were washed in 2% FBS in PBS, blocked with 2% human AB serum in PBS, then stained with a cocktail of fluorescently labeled monoclonal antibodies for 20 min on ice (see Supplemental Information for antibodies used). Labeled cells were washed with PBS and resuspended in 2% FBS/PBS prior to flow cytometric analysis. FACSymphony equipped with FACSDiva Software (BD Biosciences) was used to assess cell surface expressions and FlowJo Software was used for the analysis. Dead cells were excluded based on LIVE/DEAD^{TM} Fixable Violet Dead Cell Stain (FVD, Invitrogen, cat# L34955). For EC co-cultures, ECs were excluded by gating on CD45+ cells or CD45+CD144- cells.

A fraction of the C/G-CB cells isolated from xenograft models or cultured in EC co-culture or MC at various timepoints were sent to Hematologics, Inc (Seattle, WA) for assessment of the RAM immunophenotype along with C/G patient samples.

Histology and immunocytochemistry

Sample tissues were fixed in 10% formalin, processed into paraffin sections and stained with hematoxylin and eosin (H&E). Immunohistochemistry was performed using antibodies to ERG (EP111; Cell Marque) and CD56 (MRQ-42; Cell Marque) following citrate pretreatment and visualized with 3, 3'-diaminobenzidine (DAB) on a Ventana Bench Mark Ultra.

All tissues were examined by a board certified Hematopathologist (KRL). The bone marrow core biopsy specimen was fixed in acetic acid-zinc-formalin (AZF), decalcified, and embedded in paraffin, and sections were stained for CD56 (clone MRQ-42; Cell Marque, Rockin, California).

RNA-seq analysis

RNA-sequencing Library Construction. Total RNA was extracted using the QIAcube automated system with AllPrep DNA/RNA/miRNA Universal Kits (QIAGEN, Valencia, CA, #80224) for diagnostic pediatric AML samples from peripheral blood or bone marrow, as well as, bulk healthy bone marrows, and healthy CD34+ peripheral blood samples. Total RNA from C/G-CB and GFP-CB cells in EC co-culture and MC at indicated timepoints was purified as described above. The 75bp strand-specific paired-end mRNA libraries were prepared using the ribodepletion 2.0 protocol by the British Columbia Genome Sciences Center (BCGSC, Vancouver, BC) and sequenced on the Illumina HiSeq 2000/2500. Sequenced reads were quantified using Kallisto v0.45.0[30] with a GRCh38 transcriptome reference prepared using the coding and noncoding transcript annotations in in Gencode v29 and RepBase v24.01 and gene-level counts and abundances were produced using tximport v1.16.1[31].

Screening of C/G Fusion in patient samples. The *C/G* fusion transcript was detected by Fragment length analysis or fusion detection algorithms STAR-fusion v1.1.0 and TransAbyss v1.4.10[32,33]. Details of the procedure are described previously[4].

Transcriptome Analysis: Differentially expressed genes between C/G-CB and GFP-CB cells were identified using the limma voom (v3.44.3 R package) with trimmed mean of M values (TMM) normalized gene counts[34]. Genes with absolute log2 fold-change > 1 and Benjamini–Hochberg adjusted p-values < 0.05 were retained. Unsupervised hierarchical clustering was completed using the ComplexHeatmap R package (v2.4.3), utilizing Euclidean distances with the ward.D2 linkage algorithm. Log2 transformed TMM normalized counts per million (CPM) were used as input, with a count of 1 added to avoid taking the log of zero. Hierarchical clustering of primary C/G AML samples and C/G-CB cells using a C/G transcriptome signature was carried out. The signature genes (N=1,116 genes) were defined as those within the 75th percentile of absolute log2 fold-changes and adj. p.value < 0.001, when

contrasting C/G fusion positive patients (N=39) against a heterogenous AML reference cohort (N=1,355). The 85th percentile of this signature (N = 167 genes) was used to define a C/G gene set in GSEA.

Gene-set enrichment scores were calculated using the single-sample gene-set enrichment (ssGSEA) method (GSVA v1.32.0), which transforms normalized count data from a gene by sample matrix to a gene-set by sample matrix[35]. Counts were TMM normalized and log2(x+1) transformed prior to gene-set analysis. Curated signaling and metabolic gene-sets from the KEGG database were included in the analysis (gageData v2.26.0). Significant gene-sets (Benjamini–Hochberg adjusted p-values < 0.05) associated with C/G-CB cells were identified using limma v3.44.3 with the GSVA transformed gene-set by sample matrix as input.

GSEA was performed using the 'unpaired' comparison in the GAGE R package (v2.38.3), which tests for differential expression of gene-sets by contrasting C/G-CB against GFP-CB cells in each condition to define pathways enriched in EC co-culture versus MC. Non-redundant gene-sets were extracted for further analysis, followed by the identification of core genes that contribute to the pathway enrichment. Gene-sets from the Molecular Signatures Database (MSigDB) and the KEGG pathway database were used. Enrichment score plots for the HSC and C/G signatures were generated using the R package fgsea (v1.14.0). Log fold change values obtained from limma (contrasting C/G-CB EC week 6 against C/G-CB MC week 6) were used as a ranking metric for genes in the two signatures.

Unsupervised clustering of C/G-CB cells with pediatric AML primary diagnostic samples (N=1,033) and healthy normal bone marrows (N=68) was performed by uniform manifold approximation and projection (UMAP) using the uwot v0.1.8 R package[36]. For UMAP clustering, gene counts underwent variance stabilizing transformation (VST) using the DESeq2 v1.28.1 package. Input genes for clustering (N=6,678 genes) were selected using the mean versus dispersion parametric model trend (SeqGlue v0.1) to identify genes with high variability.

Identification of fusion-specific CAR targets involves three main steps: 1) Determine the ratio of expression for AML primary samples versus healthy normal hematopoietic tissue samples (bulk normal bone marrow, N=68, in combination with CD34+ selected peripheral blood samples, N=16) from log10 transformed normalized expression as transcripts per million, (TPM). Normalization was completed on the full gene expression matrix followed by ratio analysis on 19,901 annotated protein-coding genes for the identification of therapeutic targets. The ratio is calculated per gene from the mean expression in AML and normal tissues, where normal healthy hematopoietic tissue mean expression is the divisor, which acts as a measure of over or under expression. A normal curve is fit to the ratio values, and genes with ratios greater than +2 standard deviations were retained. This process is carried out for all heterogenous AML samples (N=1483) as a group and then repeated iteratively within AML fusion and mutation subtypes, including C/G, to ensure the inherent variability of gene expression in different fusion classes is addressed and all viable targets are identified for any given subtype. Genes are then further refined to include those with maximum expression < 1.0 TPM in normal healthy hematopoietic tissue samples, and thus considered to have AML restricted expression when compared to healthy controls. 2) AML restricted genes were further selected if found to be significantly overexpressed by RNA-seq for bulk fusion positive patient samples compared to bulk healthy bone marrows and were likewise overexpressed in C/G-CB at weeks 6 and 12 in EC co-culture with an absence of expression (< 1.0 TPM) in GFP-CB controls providing several candidate targets. 3). Final selection of optimal CAR-T targets was determined by the identification of candidate genes with cell surface localization potential as annotated by the Human Protein Atlas (https://www.proteinatlas.org/) or Jensen Lab compartments database (https://compartments.jensenlab.org/), in addition to having moderate to high expression in C/G patient samples (maximum expression ≥ 10 TPM), expression in a majority (> 75%) of patient samples, and an absence of expression in healthy hematopoietic tissues as noted in step 1 above.

Generation of human FOLR1 CAR T cells

CAR T cells were generated by transducing healthy donor T cells (Bloodworks Northwest) with lentivirus carrying the FOLR1 CAR vectors. Peripheral blood mononuclear cells from healthy donors were isolated over Lymphoprep (StemCell Technologies, Cat# 07851). CD4 or CD8 T cells were isolated by negative magnetic selection using Easy Sep Human CD4+ T cell Isolation Kit II (StemCell Technologies, Cat # 17952) and Easy Sep Human CD8+ T cell Isolation Kit II (StemCell Technologies, Cat # 17953). Purified T cells were cultured in CTL media [RPMI supplemented with 10% Human serum (Bloodworks Northwest), 2% L-glutamine (Gibco, Cat# 25030-081 1% pen-strep (Gibco, Cat#15140-122), 0.5 M beta-mercaptoethanol (Gibco, Cat# 21985-023), and 50 U/ml IL-2 (aldesleukin, Prometheus)] at 37°C in 5% CO_2. T cells were activated with anti-CD3/CD28 beads (3:1 beads: cell, Gibco,

11131D) on Retronectin-coated plates (5 ug/mL, coated overnight at 4°C; Takara, Cat# T100B) and transduced with CAR lentivirus (MOI = 50) one day after activation via spinoculation at 800g for 90 min at 25°C in CTL media (+50 U/mL IL-2) supplemented with 8ug/mL protamine sulfate. Transduction used 200,000 cells per well in 24-well plates. Transduced cells were expanded in CTL media (+50 U/mL IL-2) and separated from beads on day 5. As truncated CD19 was co-expressed with the CAR by a T2A ribosomal skip element, it was used to select for transduced cells. Transduced cells were sorted for CD19 expression [using anti-human CD19 microbeads (Miltenyi Biotec, Cat# 130-050-301)] on Automacs 8-10 days post activation. Sorted cells were further expanded in CTL (+50 U/mL IL-2) media for an additional 4-6 days prior to *in vitro* and *in vivo* cytotoxicity assays.

In vitro cytotoxicity studies

Target cells (C/G-CB >9 weeks in EC co-culture, M07e, WSU-AML, Kasumi-1 *FOLR1*+ and Kasumi-1 parental) were split 1-2 days prior to cytotoxicity assay. Target leukemia cells were labeled with 2.5 uM CFSE (Invitrogen, Cat # C34554) per manufacturer's protocol, washed with 1X PBS, and resuspended in CTL media (without IL-2). For T cell proliferation assay, effector cells (unmodified or CAR T cells) were labeled with 2.5 uM Violet Cell Proliferation Dye (Invitrogen, Cat # C34557) washed with 1X PBS, serial diluted in CTL media (without IL-2) and combined with target cells at various effector:target (E:T) ratios in 96-well U-bottom plate. Cytotoxicity (at indicated time points) and T cell proliferation (4 days) were assessed by flow cytometry after staining cells with live/dead fixable viability dyes [FVD; Invitrogen, Cat# L34964 (cytotoxicity) or L10120 (T cell proliferation)]. Percent dead amongst target cells was assessed by gating on FVD+ amongst CFSE+ target cells. Percent specific lysis was calculated by subtracting the average of the three replicate wells containing target cells only from each well containing target and effector cells at each E:T ratio. After 24 hours of co-culture, media supernatant was assessed for IL-2, IFN-γ, and TNF-α production by Luminex microbead technology (provided by FHCRC Immune Monitoring Core).

Optimization of IgG4 spacer region for efficient CAR T activity

To evaluate the therapeutic potential of targeting FOLR1, we generated FOLR1-directed CARs by fusing the single-chain variable fragment (scFv) derived from anti-FOLR1 antibody Farletuzumab to the IgG4 spacer, CD28 transmembrane, 4-1BB co-stimulatory and CD3z signaling domains (Supplemental Fig. 4a). We optimized the IgG4 spacer region against fusion-positive cells lines (M0-7e and WSU-AML), C/G-CB cells, Kasumi-1 cells engineered to express FOLR1 (Kasumi-1 *FOLR1+*) and Kasumi-1 parental cells (Supplemental Fig. 4b). Although all constructs conferred similar cytotoxicity against FOLR1+ cells, intermediate spacer CAR produced higher levels of proinflammatory cytokines (IL-2, IFN-g and TNF-a) compared to short and long IgG4 spacers (Supplemental Fig. 4c, d). We assayed NFAT, NFkB and AP-1 expression in Jurkat Nur77 reporter cells[25] transduced with the CAR constructs either cultured alone or co-cultured with Kasumi-1 *FOLR1+* cells. None of the FOLR1 CAR constructs demonstrated tonic signaling in the absence of target binding (Supplemental Fig. 4e, f).

In vivo cytotoxicity studies

Target leukemia cells were transduced with mCherry/ffluciferase (C/G-CB, weeks 9-12 in EC co-culture; Plasmid #104833, Addgene) or eGFP/ffluciferase construct (WSU-AML, Kasumi-1 *FOLR1*+ and Kasumi-1 parental; Plasmid #104834, Addgene) and sorted for mCherry+ or GFP+ cells, respectively. Luciferase-expressing cells were injected intravenously into NSG-SGM3 (C/G-CB) at $5x10^6$ cells per mouse or NSG (WSU-AML, Kasumi-1 *FOLR1*+ and Kasumi-1 parental) mice at $1x10^6$ cells through the tail vein. Mice were treated with FOLR1 CAR T or unmodified T cells via tail vein intravenous injection one week following leukemia cell injection. Leukemia burden was measured by bioluminescence imaging weekly. Leukemia burden and T cell expansion were monitored by flow cytometric analysis of mouse peripheral blood, which was drawn by retro-orbital bleeds for the indicated time points starting from the first week of T cell injection. Flow cytometric analysis of peripheral blood and tissues was performed as described above (see Supplemental information for antibodies).

Colony-forming cell assay

Following 6 and 12 weeks of culture, cells were placed in or Megacult (Megacult-C, Collagen & Medium with Cytokines Stemcell Technologies, Cat #04961) and incubated at 37°C in 5% CO_2 for 10-14 days. Colonies from megacult cultures were fixed in 3.7% formaldehyde, and then washed in PBS, and stained with MegaCult™-C Staining Kit for CFU-Mk (StemCell Technologies Cat# 04962) per manufacturer's instructions; or were permeabilized after fixation in 0.1% Triton X-100 for 10min, blocked in in 1% BSA in

PBST(PBS+0.1% Tween-20) for 30min, then stained with biotin-conjugated mouse anti-human CD41 (Biolegend, cat# 303734) and FITC-conjugated goat anti-GFP(abcam, cat# ab6662) followed by secondary stain with Alexa 647-labeled Streptavidin (Biolegend, cat# 405237) per manufacturer's instructions, and colonies were stained with DAPI prior to imaging using the TissueFAX microscope. Mk colonies were scored based on positive staining for CD41 and enumerated.

C/G-CB and normal HPSCs after co-cultured with unmodified or CAR T cells for 4 hours were placed in Methocult H4034 Optimum (Stemcell Technologies, Cat #04034). Colonies derived from erythroid (E), granulocyte-macrophage (G, M, and GM) and multipotential granulocyte, erythroid, macrophage, megakaryocyte (GEMM) progenitors were scored and enumerated after 7-10 days as directed by manufacturer's instructions.

Statistical analysis for *in vitro* and *in vivo* studies

Unpaired, two-tailed Student's t test was used to determine statistical significance for all *in vitro* studies. Log-rank (Mantel-Cox) test was used to compare Kaplan-Meier survival curves between experimental groups. Statistical significance is defined for $p<0.05$.

Data and code Availability

RNA-seq data on primary patient samples are deposited in GDC, SRA and Target Data Matrix. RNA-seq data on engineered CB are deposited in GEO. All codes used in this are publicly available.

Declarations

Acknowledgment

This study was supported by Project StElla, NCI (National Cancer Institute) TARGET, and Target Pediatric AML (TpAML) initiatives.

Authorship

Contribution: Q.L. designed the experiments; Q.L, T.H., J.S., A.L., B.J.H, T.H., S.C., T.T., C.M., LaKeisha P., Laura P., J.S., A.B., R.W., R.I., S.F., T.I., L.C. and R.R. performed the experiments and analyzed the data; S.S., S.I, M.L., L.B, S.R., I.D.B. and K.T. provided general scientific guidance. Q.L., B.H., K.L. and S.M. wrote the manuscript. All authors reviewed the manuscript prior to submission.

Conflict-of-interest disclosure: Laura P, L.B. and M.R.L. are employees of Hematologics and M.R.L. has equity ownership in Hematologics, Inc. All other authors declare no competing financial interests.

References

1 de Rooij, J. D. *et al.* Pediatric non-Down syndrome acute megakaryoblastic leukemia is characterized by distinct genomic subsets with varying outcomes. *Nat Genet* **49**, 451-456, doi:10.1038/ng.3772 (2017).

2 Gruber, T. A. *et al.* An Inv(16)(p13.3q24.3)-encoded CBFA2T3-GLIS2 fusion protein defines an aggressive subtype of pediatric acute megakaryoblastic leukemia. *Cancer Cell* **22**, 683-697, doi:10.1016/j.ccr.2012.10.007 (2012).

3 Masetti, R. *et al.* CBFA2T3-GLIS2 fusion transcript is a novel common feature in pediatric, cytogenetically normal AML, not restricted to FAB M7 subtype. *Blood* **121**, 3469-3472, doi:10.1182/blood-2012-11-469825 (2013).

4 Smith, J. L. *et al.* Comprehensive Transcriptome Profiling of Cryptic CBFA2T3-GLIS2 Fusion-Positive AML Defines Novel Therapeutic Options: A COG and TARGET Pediatric AML Study. *Clin Cancer Res* **26**, 726-737, doi:10.1158/1078-0432.CCR-19-1800 (2020).

5 Bolouri, H. *et al.* Publisher Correction: The molecular landscape of pediatric acute myeloid leukemia reveals recurrent structural alterations and age-specific mutational interactions. *Nat Med* **25**, 530, doi:10.1038/s41591-019-0369-7 (2019).

6 Pardo, L. M. *et al.* Deciphering the Significance of CD56 Expression in Pediatric Acute Myeloid Leukemia: A Report from the Children's Oncology Group. *Cytometry B Clin Cytom* **98**, 52-56, doi:10.1002/cyto.b.21829 (2020).

7 Eidenschink Brodersen, L. *et al.* A recurrent immunophenotype at diagnosis independently identifies high-risk pediatric acute myeloid leukemia: a report from Children's Oncology Group. *Leukemia* **30**, 2077-2080, doi:10.1038/leu.2016.119 (2016).

8 Thirant, C. *et al.* ETO2-GLIS2 Hijacks Transcriptional Complexes to Drive Cellular Identity and Self-Renewal in Pediatric Acute Megakaryoblastic Leukemia. *Cancer Cell* **31**, 452-465, doi:10.1016/j.ccell.2017.02.006 (2017).

9 Paredes-Aguilera, R., Romero-Guzman, L., Lopez-Santiago, N. & Trejo, R. A. Biology, clinical, and hematologic features of acute megakaryoblastic leukemia in children. *Am J Hematol* **73**, 71-80, doi:10.1002/ajh.10320 (2003).

10 Bertuccio, S. N. *et al.* The Pediatric Acute Leukemia Fusion Oncogene ETO2-GLIS2 Increases Self-Renewal and Alters Differentiation in a Human Induced Pluripotent Stem Cells-Derived Model. *Hemasphere* **4**, e319, doi:10.1097/HS9.0000000000000319 (2020).

11 Pinho, S. & Frenette, P. S. Haematopoietic stem cell activity and interactions with the niche. *Nat Rev Mol Cell Biol* **20**, 303-320, doi:10.1038/s41580-019-0103-9 (2019).

12 Poulos, M. G. *et al.* Activation of the vascular niche supports leukemic progression and resistance to chemotherapy. *Exp Hematol* **42**, 976-986 e971-973, doi:10.1016/j.exphem.2014.08.003 (2014).

13 Walter, R. B. *et al.* Heterogeneity of clonal expansion and maturation-linked mutation acquisition in hematopoietic progenitors in human acute myeloid leukemia. *Leukemia* **28**, 1969-1977, doi:10.1038/leu.2014.107 (2014).

14 Le, Q., Hadland, B., Meshinchi, S. & Bernstein, I. Notch blockade overcomes endothelial cell-mediated resistance of FLT3/ITD-positive AML progenitors to AC220 treatment. *Leukemia*, doi:10.1038/s41375-020-0893-y (2020).

15 Butler, J. M. *et al.* Development of a vascular niche platform for expansion of repopulating human cord blood stem and progenitor cells. *Blood* **120**, 1344-1347, doi:10.1182/blood-2011-12-398115 (2012).

16 Imren, S. *et al.* Modeling de novo leukemogenesis from human cord blood with MN1 and NUP98HOXD13. *Blood* **124**, 3608-3612, doi:10.1182/blood-2014-04-564666 (2014).

17 Welch, J. J. *et al.* Global regulation of erythroid gene expression by transcription factor GATA-1. *Blood* **104**, 3136-3147, doi:10.1182/blood-2004-04-1603 (2004).

18 Wang, X. *et al.* Control of megakaryocyte-specific gene expression by GATA-1 and FOG-1: role of Ets transcription factors. *EMBO J* **21**, 5225-5234, doi:10.1093/emboj/cdf527 (2002).

19 Vyas, P., Ault, K., Jackson, C. W., Orkin, S. H. & Shivdasani, R. A. Consequences of GATA-1 deficiency in megakaryocytes and platelets. *Blood* **93**, 2867-2875 (1999).

20 Shivdasani, R. A., Fujiwara, Y., McDevitt, M. A. & Orkin, S. H. A lineage-selective knockout establishes the critical role of transcription factor GATA-1 in megakaryocyte growth and platelet development. *EMBO J* **16**, 3965-3973, doi:10.1093/emboj/16.13.3965 (1997).

21 Kuhl, C. *et al.* GATA1-mediated megakaryocyte differentiation and growth control can be uncoupled and mapped to different domains in GATA1. *Mol Cell Biol* **25**, 8592-8606, doi:10.1128/MCB.25.19.8592-8606.2005 (2005).

22 Scaranti, M., Cojocaru, E., Banerjee, S. & Banerji, U. Exploiting the folate receptor alpha in oncology. *Nat Rev Clin Oncol* **17**, 349-359, doi:10.1038/s41571-020-0339-5 (2020).

23 Dang, J. *et al.* AMKL chimeric transcription factors are potent inducers of leukemia. *Leukemia* **31**, 2228-2234, doi:10.1038/leu.2017.51 (2017).

24 Gilliland, D. G. Hematologic malignancies. *Curr Opin Hematol* **8**, 189-191, doi:10.1097/00062752-200107000-00001 (2001).

25 Rosskopf, S. *et al.* A Jurkat 76 based triple parameter reporter system to evaluate TCR functions and adoptive T cell strategies. *Oncotarget* **9**, 17608-17619, doi:10.18632/oncotarget.24807 (2018).

26 Dull, T. *et al.* A third-generation lentivirus vector with a conditional packaging system. *J Virol* **72**, 8463-8471 (1998).

27 Turtle, C. J. *et al.* Immunotherapy of non-Hodgkin's lymphoma with a defined ratio of CD8+ and CD4+ CD19-specific chimeric antigen receptor-modified T cells. *Sci Transl Med* **8**, 355ra116, doi:10.1126/scitranslmed.aaf8621 (2016).

28 Delaney, C. *et al.* Notch-mediated expansion of human cord blood progenitor cells capable of rapid myeloid reconstitution. *Nat Med* **16**, 232-236, doi:10.1038/nm.2080 (2010).

29 Butler, J. M. *et al.* Endothelial cells are essential for the self-renewal and repopulation of Notch-dependent hematopoietic stem cells. *Cell Stem Cell* **6**, 251-264, doi:10.1016/j.stem.2010.02.001 (2010).

30 Bray, N. L., Pimentel, H., Melsted, P. & Pachter, L. Near-optimal probabilistic RNA-seq quantification. *Nat Biotechnol* **34**, 525-527, doi:10.1038/nbt.3519 (2016).

31 Soneson, C., Love, M. I. & Robinson, M. D. Differential analyses for RNA-seq: transcript-level estimates improve gene-level inferences. *F1000Res* **4**, 1521, doi:10.12688/f1000research.7563.2 (2015).

32 Haas, B. J. *et al.* Accuracy assessment of fusion transcript detection via read-mapping and de novo fusion transcript assembly-based methods. *Genome Biol* **20**, 213, doi:10.1186/s13059-019-1842-9 (2019).

33 Robertson, G. *et al.* De novo assembly and analysis of RNA-seq data. *Nat Methods* **7**, 909-912, doi:10.1038/nmeth.1517 (2010).

34 Ritchie, M. E. *et al.* limma powers differential expression analyses for RNA-sequencing and microarray studies. *Nucleic Acids Res* **43**, e47, doi:10.1093/nar/gkv007 (2015).

35 Hanzelmann, S., Castelo, R. & Guinney, J. GSVA: gene set variation analysis for microarray and RNA-seq data. *BMC Bioinformatics* **14**, 7, doi:10.1186/1471-2105-14-7 (2013).

36 Leland McInnes, J. H., James Melville. UMAP: Uniform ManifoldApproximation and Projection forDimension Reduction. *arxiv*, doi: arXiv:1802.03426 (2020).

Figures

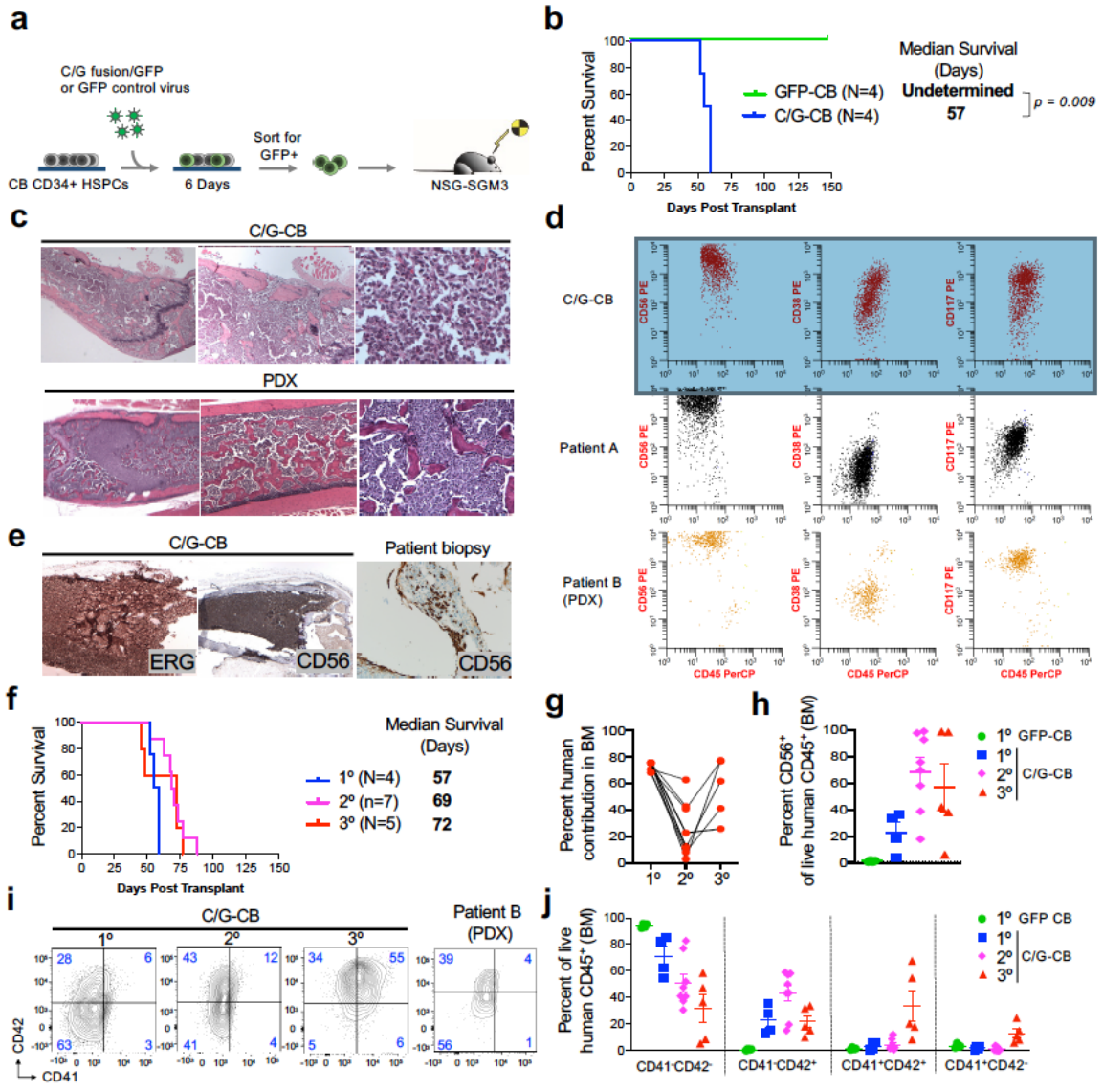

Figure 1

C/G-CB cells induce leukemia recapitulating primary disease. a. Diagram of experimental design. b. Kaplan-Meier survival curves of NSG-SGM3 mice transplanted with GFP-CB control and C/G-CB cells. Statistical differences in survival were evaluated using Log-rank Mantel-Cox. c. Representative histology of H&E stain of femurs taken from mice transplanted with C/G-CB cells (top) and a C/G positive patient sample (bottom) after development of leukemia. Magnification: left (2.5X), middle (5X), Right (C/G-CB 40X; PDX, 20X). d. Expression of the RAM immunophenotype in C/G-CB cells harvested from the bone marrow of a representative mouse at necropsy compared to a primary patient sample and PDX marrow xenograft cells. In all three samples, malignant cells were gated based on human CD45 expression and SSC. e. Left and middle, representative immunohistochemistry showing high expression of ERG (10X magnification) and CD56 (5X magnification) in the femur of a representative mouse transplanted with C/G-CB cells. Right, small aggregates of blasts with high CD56 expression detected in a bone marrow biopsy of a chemotherapy refractory C/G fusion positive patient, consistent with residual, adherent, patchy disease distribution (100X magnification). f. Kaplan-Meier plot showing survival in primary (1°), secondary (2°) and tertiary (3°) transplantations of C/G-CB cells. g. Engraftment of C/G-CB cells in the bone marrow at time of symptomatic leukemia, shown as percent human CD45+. h. Quantification of CD56+ cells amongst human CD45+ cells isolated from the bone marrow (BM) at necropsy following development of symptomatic leukemia. i. Expression of AMKL markers, CD41 and CD42, in C/G-CB and PDX cells harvested from the bone marrow at necropsy.

C/G-CB cells were gated on human CD45+ cells. PDX cells were gated on human CD45+CD56+ cells. j. Quantification of CD41/CD42 subsets described in i. Bars indicate mean +/- SEM.

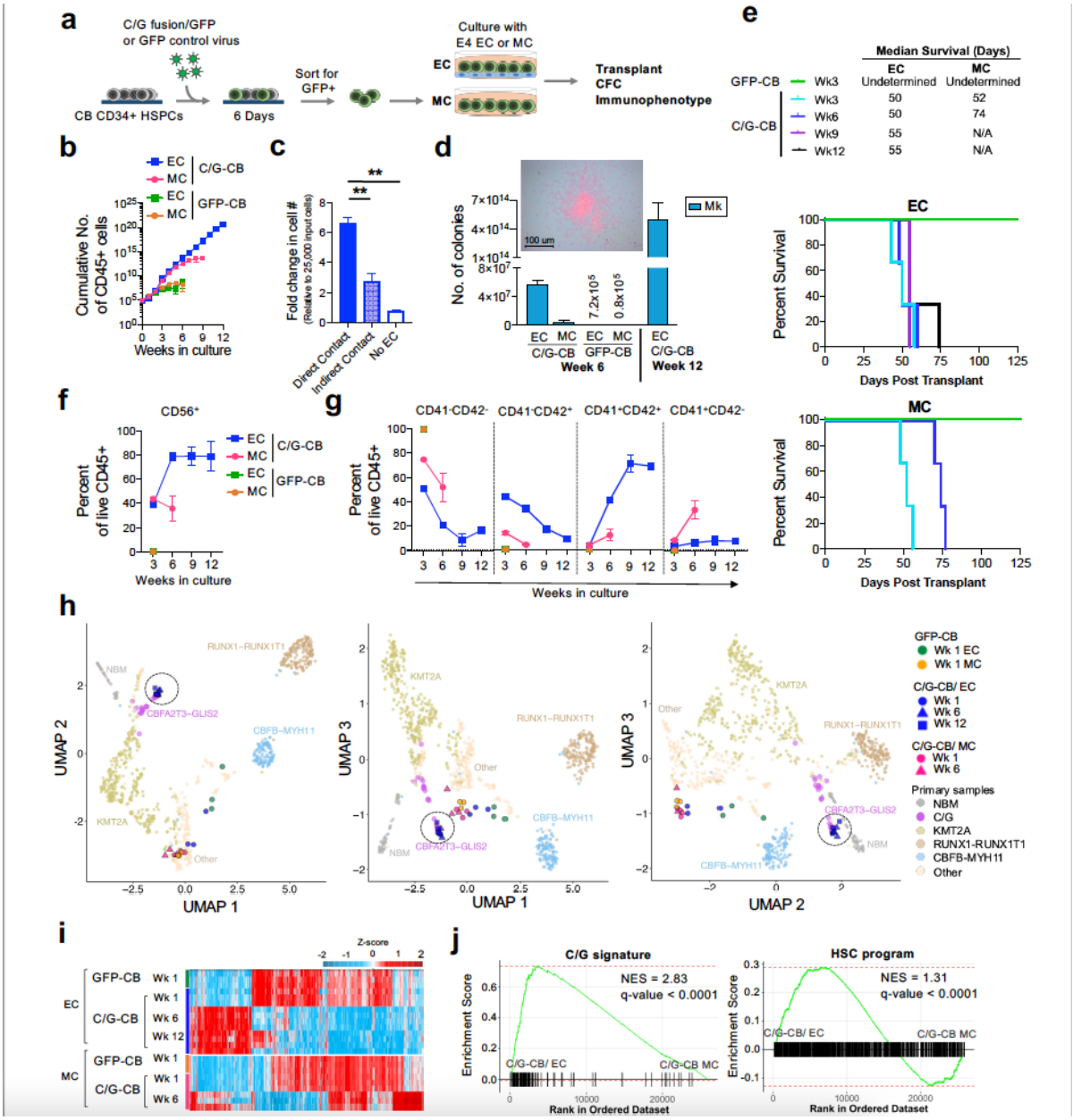

Figure 2

ECs enhance the proliferative potential and promote leukemic progression of C/G-CB cells. a. Diagram of experimental design. b. Growth kinetics of C/G-CB and GFP-CB cells in EC co-culture or MC. c. C/GCB cells expanded in EC co-culture for 9 weeks were reseeded in EC co-culture either directly (direct contact) or in EC transwells (indirect contact) or placed in liquid culture containing SFEM II (+SCF, FLT3L, and TPO). After 7 days, the number of GFP+ cells was quantified by flow cytometry. d. At 6 and 12 weeks, a fraction of each culture was transferred to MegaCult cultures. Colonies derived from megakaryocytic (Mk) progenitors were scored and enumerated. Data are normalized to the 500 input cells at the start of the EC co-culture or MC culture. A representative colony stained with anti-human CD41 and an alkaline phosphotase detection system is shown. e. Equivalent number of C/G-CB and GFP-CB cells were transplanted into NSG-SGM3 mice (5-10x106/mouse) at indicated timepoints. Due to insufficient expansion, GFP-CB cells were not transplanted after 3 weeks in either condition, similarly for C/G-CB cells after 6 weeks in MC culture. Median survival and Kaplan-Meier survival curve are shown. C/G-CB (N=3 mice/group), GFP-CB (N=2 mice/group) f, g. Quantification of CD56+ cells (f) and CD41/CD42 subsets (g) amongst human CD45+ cells over weeks in culture. h. Unsupervised clustering by uniform manifold and projection (UMAP) analysis of C/G-CB and GFP-CB cells in reference to primary AML samples. Dashed circle indicates C/G-CB cells co-cultured with ECs at week 6 and 12 timepoints. NBM=normal bone marrow. i. Heatmap of differentially expressed genes in

C/G-CB versus GFP-CB cells in EC co-culture or MC. j. GSEA plots of C/G and HSC signature genes comparing C/G-CB cells in EC co-culture versus MC. (b-e, g-i) Data presented as mean +/- standard deviation from 3 technical replicates.

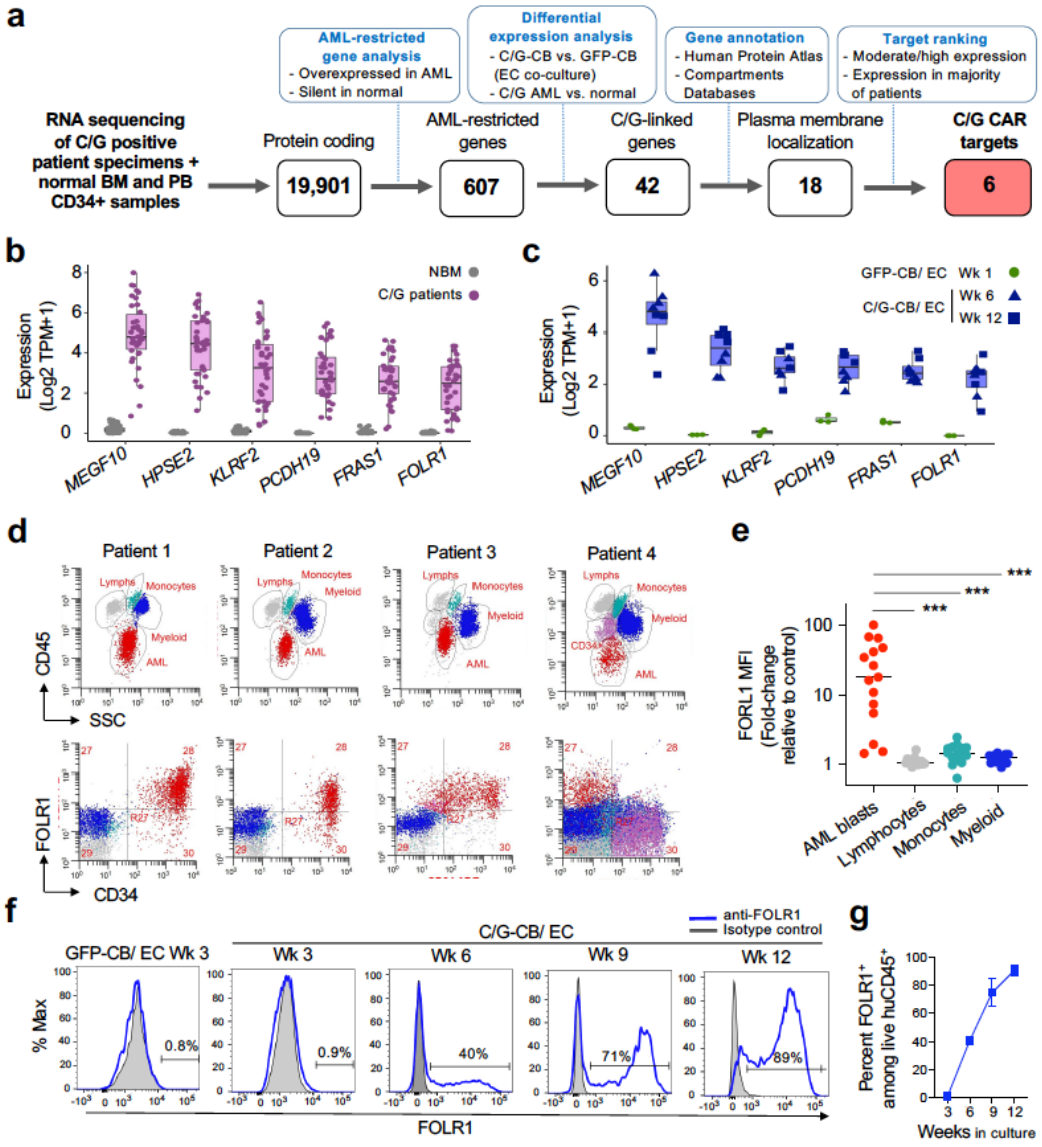

Figure 3

Integrative transcriptomics of primary samples and C/G-CB identify FOLR1 therapeutic target. a. Diagram of computational workflow to identify C/G-specific CAR targets. See Methods and Extended Data Fig. 7 for details. Normal tissues include bulk bone marrow (BM) samples and peripheral blood (PB) CD34+ samples. b, c. Expression of C/G-specific CAR targets in primary fusion positive patients versus normal bone marrow (NBM) (b) and C/G-CB versus GFP-CB cells (c). d. Top, gating strategies used to identify AML cells and normal lymphocytes, monocytes and myeloid cells in 4 representative patients based on CD45 expression and SSC. Bottom, FOLR1 expression in the AML blast subpopulation versus normal cells. e. Quantification of FOLR1 expression (geometric mean fluorescent intensity, MFI) among AML blasts and their normal counterparts across N=15 patients. Autofluorescence was used as control. ***, p<0.0005 (paired Student t-test) f, g. Expression of FOLR1 (f) and quantification of FOLR1+ cells (g) amongst GFP-CB and C/G-CB over weeks in EC co-culture.

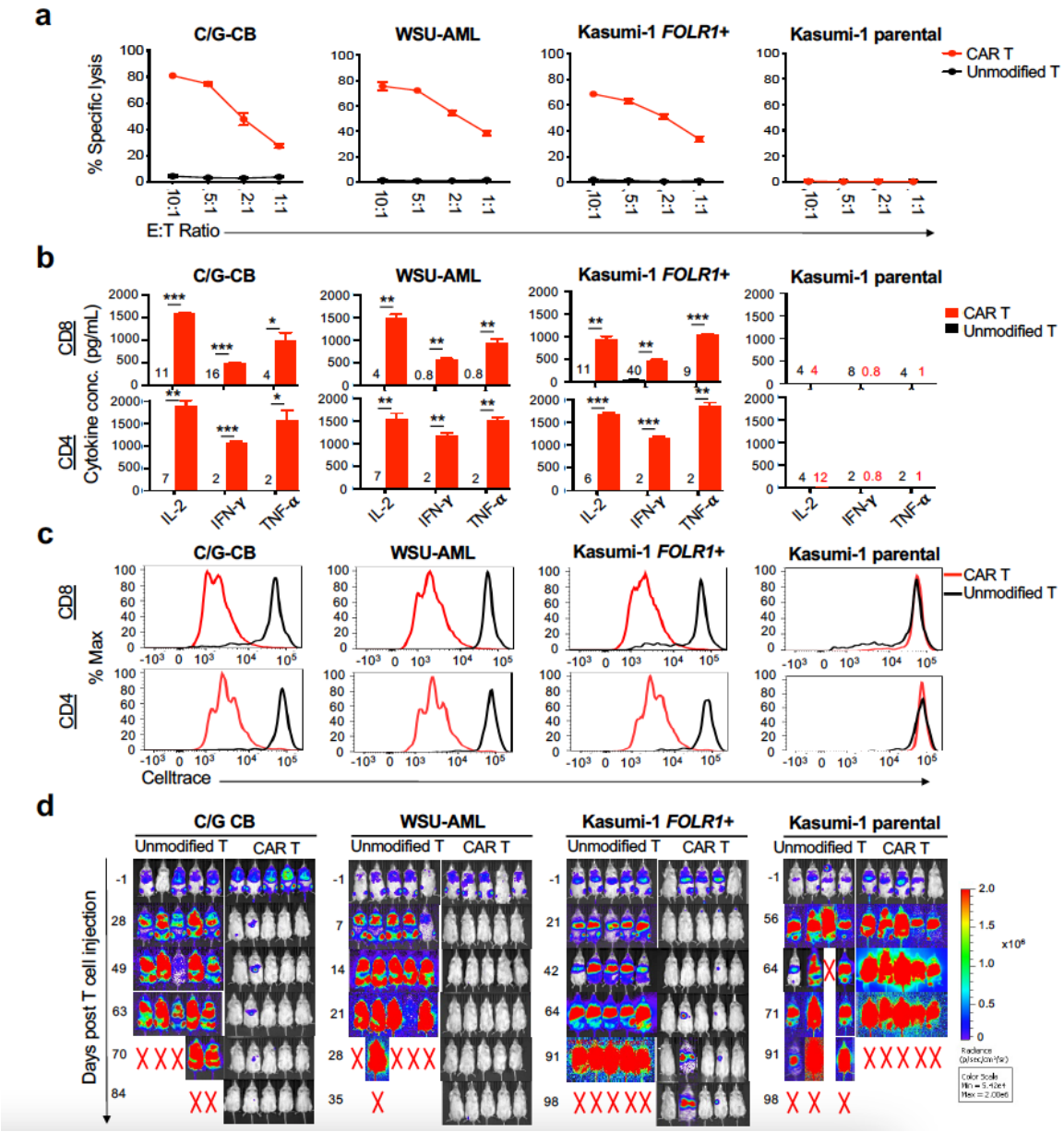

Figure 4

Pre-clinical efficacy of FOLR1 CAR T cells against C/G AML cells. a. Cytolytic activity of CD8 T cells unmodified or transduced with FOLR1 CAR following 6 hours of co-culture with C/G-CB, WSU-AML, Kasumi-1 FOLR1+ and Kasumi-1 parental cells. Data presented are mean leukemia specific lysis +/- SD from 3 technical replicates at indicated effector: target (E:T) ratios. Data are representative of 2 donors (see related data in Supplemental Fig. 3). b. Concentration of secreted IL-2, IFN-γ, and TNF-α in the supernatant following 24 hour of T cell/AML co-culture at 1:1 E:T ratio as measured by ELISA. Data are representative of 2 donors and are presented as mean +/- SD from 3 technical replicates (see related data in Supplemental Fig. 4). Where concentrations of cytokines are too low to discern, the number above the x-axis indicates the average concentration. Statistical significance was determined by unpaired Student's t test, assuming unequal variances. $p<0.05$ (*), $p<0.005$ (**), $p<0.0005$ (***). c. Representative flow cytometric analysis of cell proliferation of Cell Proliferation Dye (Celltrace)-labeled unmodified and FOLR1 CAR T cells after 4-day co-culture with target cells at 1:1 E:T ratio. CAR T cells divided rapidly and diluted their Celltrace fluorescence after 4-hour co-incubation with FOLR1-positive AML cells. Data are representative of 2 donors. d. Bioluminescent imaging of C/G-CB, WSU-AML, Kasumi-1 FOLR1+ and Kasumi-1 leukemias in mice treated with unmodified or FOLR1 CAR T cells at 5 x106 T cells per mouse. N=5 mice/group. Radiance scale indicates an increase in leukemia from blue to red; X indicates death.

Supplementary Files

This is a list of supplementary files associated with this preprint. Click to download.

- LeSupplementalInformation.pdf
- ExtendedDataFigure1.pdf
- ExtendedDataFigure2.pdf
- ExtendedDataFigure3.pdf
- ExtendedDataFigure4.pdf
- ExtendedDataFigure5.pdf
- ExtendedDataFigure6.pdf
- ExtendedDataFigure7.pdf
- ExtendedDataFigure8.pdf
- ExtendedDataFigure9.pdf